FcγRIIB Is an Immune Checkpoint Limiting the Activity of Treg-Targeting Antibodies in the Tumor Microenvironment

David A. Knorr[1,2], Lucas Blanchard[1], Rom S. Leidner[3], Shawn M. Jensen[3], Ryan Meng[3], Andrew Jones[1], Carmen Ballesteros-Merino[3], Richard B. Bell[3], Maria Baez[1], Alessandra Marino[1], David Sprott[3], Carlo B. Bifulco[3], Brian Piening[3], Rony Dahan[4], Juan C. Osorio[1,2], Bernard A. Fox[3], and Jeffrey V. Ravetch[1]

ABSTRACT

Preclinical murine data indicate that fragment crystallizable (Fc)-dependent depletion of intratumoral regulatory T cells (Treg) is a major mechanism of action of anti–CTLA-4. However, the two main antibodies administered to patients (ipilimumab and tremelimumab) do not recapitulate these effects. Here, we investigate the underlying mechanisms responsible for the limited Treg depletion observed with these therapies. Using an immunocompetent murine model humanized for CTLA-4 and Fcγ receptors (FcγR), we show that ipilimumab and tremelimumab exhibit limited Treg depletion in tumors. Immune profiling of the tumor microenvironment (TME) in both humanized mice and humans revealed high expression of the inhibitory Fc receptor, FcγRIIB, which limits antibody-dependent cellular cytotoxicity/phagocytosis. Blocking FcγRIIB in humanized mice rescued the Treg-depleting capacity and antitumor activity of ipilimumab. Furthermore, Fc engineering of antibodies targeting Treg-associated targets (CTLA-4 or CCR8) to minimize FcγRIIB binding significantly enhanced Treg depletion, resulting in increased antitumor activity across various tumor models. Our results define the inhibitory FcγRIIB as an immune checkpoint limiting antibody-mediated Treg depletion in the TME, and demonstrate Fc engineering as an effective strategy to overcome this limitation and improve the efficacy of Treg-targeting antibodies.

Introduction

Cancer immunotherapy has revolutionized the treatment of various malignancies. However, factors leading to treatment response and resistance remain poorly defined (1), and the fundamental mechanisms of these treatments are still incompletely understood (2). For anti–CTLA-4 immunotherapy, several mechanisms of action have been identified. Because CTLA-4 competes with the costimulatory receptor CD28 for the B7 ligands B7-1 (CD80) and B7-2 (CD86) to dampen T-cell activation, removal of CTLA-4–mediated negative costimulation has been accepted as the pivotal mechanism of action of anti–CTLA-4 (3). However, several murine studies have pointed toward a second mechanism of action involving the depletion of regulatory T cells (Treg) within the tumor microenviroment (TME; refs. 4–11). Tregs express high levels of CTLA-4 in the TME and their depletion is achieved through the fragment crystallizable (Fc) domain of anti–CTLA-4, resulting in reduced tumor immunosuppression and expansion of effector T cells. However, there is a lack of concrete evidence supporting Fc-mediated Treg depletion in patients receiving human anti–CTLA-4, and recent studies have demonstrated that both ipilimumab and tremelimumab fail to deplete intratumoral Tregs in patients (12). Finally, an Fc-dependent, but Treg depletion–independent, mechanism of action was recently proposed whereby anti–CTLA-4 stimulate myeloid cells that in turn activate effector T cells (13, 14).

A large proportion of the research aiming at establishing whether human anti–CTLA-4 deplete Tregs *in vivo* has relied on mouse models (5–11). However, these models present several limitations, including the differential structure, function, and expression of mouse and human Fcγ receptors (FcγR), which constitute important confounding factors (15, 16). Vargas and colleagues recently used a humanized mouse system recapitulating human FcγR structural and functional diversity to determine the contribution of the Fc domain to the *in vivo* activity of anti–CTLA-4 (8). While this study described the ability of human IgG1 antibodies to deplete Tregs in humanized models, they relied on chimeric anti–CTLA-4 [mouse fragment antigen-binding (Fab) with human Fc domain], which cannot fully recapitulate the activity of the human anti–CTLA-4 used in patients. In addition, while these studies also revealed that a combination of the FcγRIIIA high-affinity polymorphism (FcγRIIIA^{V158F}) and high tumor mutational burden could predict favorable outcomes for patients undergoing treatment with ipilimumab, these variables do not represent the majority of patients receiving anti–CTLA-4 therapy.

The inhibitory Fc receptor, FcγRIIB, is an important regulator of antibody-dependent cellular cytotoxicity/phagocytosis (ADCC/ADCP; ref. 15), which has important implications for antibody-based cancer treatments (17, 18). Therapeutic blockade of FcγRIIB has been shown to enhance ADCP of anti-CD20 in a lymphoma mouse model (19). In this setting, FcγRIIB exerts its inhibitory activity by competing with activating FcγRs for the binding of IgG antibodies, and its blockade improves the efficacy of antibody-mediated cell depletion therapy (20). Furthermore, FcγRIIB expression is induced by IL4 and

[1]Laboratory of Molecular Genetics and Immunology, Rockefeller University, New York, New York. [2]Department of Medicine, Memorial Sloan Kettering Cancer Center, New York, New York. [3]Earle A. Chiles Research Institute (a division of Providence Cancer Institute), Portland, Oregon. [4]Department of Immunology, Weizmann Institute of Science, Rehovot, Israel.

Current address for D.A. Knorr: Regeneron, Inc., Tarrytown, New York.

D.A. Knorr, L. Blanchard, and R.S. Leidner contributed equally to this article.

Corresponding Author: Jeffrey V. Ravetch, Laboratory of Molecular Genetics and Immunology, Rockefeller University, 1230 York Ave, NY 10065. E-mail: ravetch@rockefeller.edu

Cancer Immunol Res 2024;12:322–33

doi: 10.1158/2326-6066.CIR-23-0389

hypoxia-inducible factors (21, 22), both of which are abundantly present in the TME (23–25), suggesting a potential role for this receptor in the resistance to antibody-based therapies.

Because of the dicrepancies between murine models and patients on the mechanisms of action of anti–CTLA-4, in particular concerning the Fc-dependent depletion of intratumoral Tregs, as well as the important structural, functional, and genetic differences of FcγRs between mice and humans, we developed a murine model humanized for CTLA-4 and FcγRs to study the capacity of fully human anti–CTLA-4 to deplete Tregs in tumors. Using this model system, we investigated whether the inhibitory activity of FcγRIIB could potentially explain the poor Treg-depleting capacity of ipilimumab. We found that FcγRIIB was highly expressed in both murine and human solid tumors and demonstrated that FcγRIIB acts as an important checkpoint limiting the activity of Treg-targeting antibodies in the TME.

Materials and Methods

Mouse strains

All mice were bred and housed at Rockefeller University Comparative Bioscience Center under specific pathogen-free conditions. All experiments were performed in compliance with institutional guidelines and were approved by the Rockefeller University Institutional Animal Care and Use Committee (IACUC). C57BL/6J [wild-type (WT)] mice were purchased from The Jackson Laboratory (stock no. 000664). Humanized CTLA-4 mice (C57BL/6 background) were obtained from James P. Allison (MD Anderson Cancer Center) and were described previously (4). In brief, transgenic mice expressing human CTLA-4 (chimeric construct containing upstream regulatory sequences required for CTLA-4 expression and in which the extracellular coding domain of mouse CTLA-4 is replaced by that of human CTLA-4) were backcrossed into *Ctla4*$^{-/-}$ mice. Humanized FcγR mice (C57BL/6 background) were previously generated in our lab and extensively characterized in previous studies (26). In brief, transgenic mice expressing human FCGR1A, FCGR2A^{R131}, FCGR2B^{I232}, FCGR3A^{F158}, and FCGR3B (under the control of their human regulatory elements) were individually crossed together to create a mouse line expressing the full repertoire of human FcγRs. These human FcγR transgenic mice were then backcrossed into FcRα$^{-/-}$ (deleted for *Fcgr2b*, *Fcgr3*, and *Fcgr4*) and *Fcgr1*$^{-/-}$ mice that lack all murine FcγRs. Humanized CTLA-4 mice were mated with humanized FcγR mice to obtain the humanized CTLA-4 and FcγR mice (referred to herein as "humanized CTLA-4/FcγR mice"). All mice used were 7–12 weeks old at time of experiment. All experiments used a mix of male and female mice.

Cell lines

MC38 cells were obtained from Kerafast (ENH204-FP; RRID: CVCL_B288), B16 cells were obtained from ATCC (CRL-6475; RRID:CVCL_0159) and MB49 and MCA-205 cells were obtained from Sigma-Aldrich (SCC148; RRID:CVCL_7076, and SCC173; RRID: CVCL_VR90). All cells were cultured inside tissue culture treated flasks with DMEM (#11995065, Thermo Fisher Scientific) with 10% FBS (#F2442, Sigma-Aldrich) and 1X penicillin-streptomycin (#15140122, Thermo Fisher Scientific) at 37°C and 5% CO_2. Cells were split twice per week and cell viability was measured using trypan blue staining in the Countess II automated cell counter (Thermo Fisher Scientific). All cells were used within 5–10 passages of thawing. Cell lines were tested for *Mycoplasma* and have not been reauthenticated.

Antibody production and Fc engineering

The variable heavy and light regions of ipilimumab (clone 10D1) and tremelimumab (clone 1121) were synthesized on the basis of their published sequences (https://drugs.ncats.io; Supplementary Table S1). The variable heavy and light regions of the anti-mouse CD4 (clone GK1.5) were synthesized on the basis of their published sequences (NCBI GenBank AAA51349.1 and AAA51350.1 for VH and VL sequences, respectively; Supplementary Table S1). The variable heavy and light regions of the anti-mouse CCR8 (clone SA214G2, BioLegend; RRID: AB_2566246) were determined by mass spectrometry (Bioinformatics Solutions Inc; Supplementary Table S1). The anti-human FcγRIIB (clone 2B6) was previously generated in our lab (Rockefeller University, New York, NY; ref. 27), and was produced by the Memorial Sloan Kettering Cancer Center Hybridoma Facility. The variable region sequences of the parental antibodies were cloned and inserted into AbVec2.0-IGHG1 expression vectors (#80795, Addgene). For the generation of human IgG1 N297A, GRLR (G236R/L328R), and GAALIE (G236A/A330L/I332E) Fc variants, site-directed mutagenesis using specific primers (Supplementary Table S2) was performed with QuickChange site-directed mutagenesis Kit II (#200523, Agilent Technologies) according to the manufacturer's instructions. Mutated plasmid sequences were validated by Sanger sequencing (Genewiz, Azenta Life Sciences). Antibodies were produced by transient cotransfection of Expi293F suspension cells (#A14635, Thermo Fisher Scientific) with heavy and light chain expression vectors. Expi293F cells were cultured in serum-free Expi293 Expression Medium (#A14635, Thermo Fisher Scientific), and transfected using ExpiFectamine 293 transfection reagent (#A14635, Thermo Fisher Scientific) according to the manufacturer's instructions. For the generation of the human IgG1 afucosylated Fc variant, 2-Deoxy-2-fluoro-L-fucose at 200 μmol/L (# MD06089, Biosynth Carbosynth) was added 1 day after transfection. In some experiments, afucosylated antibodies were produced by transfecting antibody heavy and light chain expression vectors into Expi293F Fut8$^{-/-}$ cells. These cells were generated in the lab and described in previous studies (28). Supernatants were collected 7 days after transfection, centrifuged and filtered (0.22 μmol/L). Antibodies were purified from clarified supernatants using Protein G Sepharose 4 Fast Flow (#17061801, Cytiva) according to the manufacturer's instructions. Purified antibodies were dialyzed in PBS and sterile filtered (0.22 μmol/L). Purity was assessed by SDS-PAGE and Coomassie staining, and endotoxin levels were determined (#C1500-5, Associates of Cape Cod Inc). The percentage of afucosylated forms was assessed by mass spectrometry or Luminex as described previously (28). The Fc variants used in the study do not impact antibody serum half-life as assessed previously (29, 30).

ELISA

Binding specificity, affinity, and blocking activity of human anti–CTLA-4 were determined by ELISA using recombinant human B7.1 (#10698-HCCH, Sino Biological), recombinant human CTLA-4 (#11159-HNAH, Sino Biological), and recombinant human FcγRs (human FCGR2A #10374-H08H, human FCGR2B #10259-H08H, human FCGR3A #10389-H08H, Sino Biological). Ninety-six–well ELISA Half Area High Binding plates (#675061, Greiner Bio-One) were coated overnight at 4°C with CTLA-4 (1 μg/mL), B7.1 (1 μg/mL), or human FcγRs (2 μg/mL). All sequential steps were performed at room temperature. After washing, the plates were blocked for 1 hour with 1×PBS containing 2% BSA (for CTLA-4 and B7.1) or 10% BSA (for human FcγRs), and were subsequently incubated for 2 hours with serially diluted IgGs (dilutions are indicated in the figures and were prepared in the relevant blocking solution). After washing, plates were

incubated for 1 hour with horseradish peroxidase (HRP)-conjugated anti-human IgG (#109-035-088, Jackson ImmunoResearch; RRID: AB_2337584). For the inhibition assay, after blocking nonspecific sites, plates were incubated for 1 hour with serially diluted IgGs and with 1 μg/mL of human CTLA-4-Biotin (Sino Biological, #11159-H08H-B) in 1×PBS with 2% BSA. After washing, plates were incubated for 1 hour with HRP-labeled streptavidin (#405210, BioLegend). Detection was performed using TMB (5120-0047, SeraCare Life Sciences), and reactions stopped with the addition of 0.18 mol/L sulphuric acid. Absorbance at 450 nm was immediately recorded using a SpectraMax Plus spectrophotometer (Molecular Devices), and background absorbance from negative control samples was subtracted.

Surface plasmon resonance

All experiments were performed with a Biacore T100 SPR system (GE Healthcare) at 25°C in HBS-EP buffer [10 mmol/L HEPES, pH 7.4, 150 mmol/L NaCl, 3.4 mmol/L edetic acid, 0.005% (v/v) surfactant P20]. Recombinant IgG antibodies were immobilized on Series S CM5 chips (GE Healthcare) and soluble ectodomains of recombinant human CTLA-4 were injected to the flow cells at different concentrations. Background binding to blank immobilized flow cells was subtracted and affinity constants were calculated using BIAcore T100 evaluation software (GE Healthcare) using the 1:1 Langmuir binding model.

Tumor transplantation and *in vivo* treatments

MC38, MCA-205, MB49, and B16 cells were detached using trypsin digestion from tissue culture flasks and assessed for viability (>95%). Cells were washed thrice with PBS and were resuspended in sterile cold PBS. Mice were injected in their lower abdominal flanks with 100 μL of this mixture, corresponding to 2×10^5 cells (for MB49 and B16), 5×10^5 cells (for MCA-205), or 2×10^6 cells (for MC38). Tumors were measured two to three times per week using an electronic caliper. Volume was calculated using the formula $({L_1}^2 \times L_2)/2$, where L_1 is the longest dimension. Mice were randomized into treatment groups when tumors were approximately 5 to 6 mm in diameter. Mice received treatment as described in the legend of each experiment. Humanized CTLA-4/FcγR mice were treated with 200 μg of anti–CTLA-4 or isotype control (intraperitoneal injection), and in some experiments, with 50 μg of anti-human FcγRIIB or control PBS (intratumoral injection). Humanized FcγR mice were treated with 200 μg of anti-CCR8 antibodies or isotype control (intraperitoneal injection). The human IgG1 isotype control antibody used in our studies was obtained from BioXCell (#BE0297; RRID: AB_2687817). For experiments assessing antitumor activity, mice were treated on days 0, 3, and 6 following randomization and were sacrificed when tumor reached the Rockefeller University IACUC limit (maximal tumor volume of 2,000 mm^3). For flow cytometry experiments, mice were treated on days 0 and 3 following randomization and were sacrificed 24 hours after the last injection for analysis.

Processing of mouse tissues

Tumors were dissected, cut into small pieces and transferred to gentleMACS C tubes (Miltenyi Biotec) containing enzyme mix for tough tumors (#130-096-730m, Miltenyi Biotec) in DMEM. Tumor fragments were then dissociated using the gentleMACS OctoDissociator with heaters (gentleMACS Program 37Cm_TDK_2, Miltenyi Biotec). Cell were finally filtered through a 70-μm cell strainer. Lymph nodes and spleens were removed from mice using forceps and pressed on a 40-μm cell strainer using the flat end of a syringe plunger. For spleens, red blood cell lysis was performed using Red Blood Cell Lysing Buffer (#R7757, Sigma-Aldrich).

Flow cytometry

Cells were stained for viability using eBioscience Fixable Viability Dye (#65-0866-14, Thermo Fisher Scientific). After viability staining, cells were resuspended in FACS buffer (PBS with 0.5% BSA and 2 mmol/L EDTA) and Fc blocked using human TrueStain FcX (#422304, BioLegend). Cells were incubated for 30 minutes at 4°C with antibodies to extracellular targets, then washed twice, fixed, and permeabilized using eBioscience Foxp3 Transcription Factor Staining Buffer kit (#00-5523-00, Thermo Fisher Scientific) prior to intracellular staining with antibodies to intracellular targets. For staining of human FcγRs, cells were directly incubated with antibodies to human FcγRs following viability staining. After 30 minutes incubation at 4°C, cells were then incubated with the other antibodies and processed normally.

The following anti-mouse antibodies were used: CD45-AlexaFluor 700 (clone 30-F11, Thermo Fisher Scientific; RRID: AB_891454), CD45-PerCP (clone 30-F11, BioLegend; RRID: AB_893343), CD3e-Percp-Cy5.5 (clone 17A2, BioLegend; RRID: AB_1595597), CD3e-PE-Cy7 (clone 17A2, BioLegend; RRID: AB_1732068), CD4-FITC (clone GK1.5, BioLegend; RRID: AB_312690), CD4-AlexaFluor 488 (clone GK1.5, BioLegend; RRID: AB_493520), CD8a-BV786 (clone 53-6.7, BioLegend; RRID: AB_312750), CD8a-PB (clone 53-6.7, BioLegend; RRID: AB_493426), FOXP3-PE (clone 150D, BioLegend; RRID: AB_492981), FOXP3-APC (clone FJK-16s, eBioscience; RRID: AB_469457), and CTLA-4-BV421 (clone UC10-4B9, BioLegend; RRID: AB_10901170).

The following anti-human antibodies were used: FcγRI-PE (clone 10.1, BioLegend; RRID: AB_1595539), FcγRIIIA/B-PE-Cy7 (clone 3G8, BioLegend; RRID: AB_314215), FcγRIIA-Dylight 488 (clone IV.3, produced in-house), FcγRIIB-Dylight 650 (clone 2B6, produced in-house), and CTLA-4-PE (clone L3D10, BioLegend; RRID: AB_10645522).

Samples were acquired on an Attune NxT flow cytometer (Thermo Fisher Scientific) and data were analyzed using FlowJo 10 (BD).

Human tumor tissues

Baseline oral squamous cell carcinoma 4 mm punch biopsy samples were obtained between November 2016 and August 2019 from consenting patients planned for standard-of-care surgical resection (the list of patients is provided in Supplementary Table S3), in accordance with ethical standards under a Providence Health & Services Institutional Review Board–approved clinical study protocol (IRB #16-042) at the Earle A. Chiles Research Institute, Providence Portland Medical Center, Portland, Oregon. Punch biopsy tumor tissue specimens were obtained by the surgeon in the ambulatory clinic, placed directly in formalin, and delivered to pathology for formalin-fixed paraffin-embedded (FFPE) processing and storage per routine institutional protocol. Patient consent was obtained as a prerequisite for study enrollment. Patient consent for publication is not required. The study was conducted in accordance with the Declaration of Helsinki.

Multiplex immunofluorescence staining

To prepare specimens for multiplex immunofluorescence (mIF) staining, tissue sections were cut at 4 μm from FFPE blocks. All sections on slides were deparaffinized using the Bond ER2 Leica Biosystems AR9640, followed by staining with the Leica Bond RX autostainer. The slides were stained with anti-human CD3 (dilution 1:50, clone SP7, #ab16669, Abcam; RRID: AB_443425), anti-human

FcγRIIIA/B (dilution 1:50, clone 2H7, #88251S, Cell Signaling Technology), anti-human FcγRIIB (dilution 1:2,000, clone 110, #NBP2-89364, Novus Biologicals; RRID: AB_354737), and anti-human CD68 (dilution 1:400, clone PG-M1, #GA61361-2, Dako Agilent). Antibody binding was visualized using the Opal 7-Color Manual IHC kit (#NEL811001KT, Akoya), which includes secondary anti-mouse/anti-rabbit polymer HRP, TSA-Opal reagents, and DAPI counterstain. Tissue slides were coverslipped with VectaShield mounting media (#H-1000-10, Vector Labs). Control tissue samples were stained for each marker as positive controls. Whole slide digital images were captured with the PhenoImager HT platform and analyzed with QuPath software. Tissue samples from consecutive slides were stained with hemtoxylin and eosin (H&E), and scanned with the Leica SCN400F platform. Tumor regions were annotated by an expert pathologist based on H&E slides in conjunction with Cytokeratin staining (clone AE1/AE3, Thermo Fisher Scientific; RRID: AB_1834350). Cells were segmented, phenotyped, and enumerated using the QuPath object classification algorithm.

Statistical analysis

Data were analyzed using Prism GraphPad software (version 9.3.1). One-way ANOVA with Tukey *post hoc* test was used to compare all groups with three or more treatments. When two groups were compared, an unpaired two-tailed Student *t* test was used to determine statistical significance. When data were not normally distributed, nonparametric tests were used: Kruskal–Wallis with Dunn *post hoc* test for multiple comparisons or Mann–Whitney test when two groups were compared. All data, unless otherwise indicated, are plotted as mean ± SEM. For all statistical tests, *, $P < 0.05$; **, $P < 0.01$; ***, $P < 0.001$; ****, $P < 0.0001$, and not significant values are denoted as ns. Lines associated with asterisks indicate groups compared for significance.

Data availibility

Data were generated by the authors and are available in the article and its Supplementary Data files or from the corresponding author upon reasonable request.

Results

A humanized mouse model to study the Fc effector function of human anti–CTLA-4

The importance of Fc-dependent mechanisms for the antitumor activity of therapeutic antibodies has been demonstrated for several targets in recent years (31–36), resulting in the development and evaluation of second-generation Fc-engineered antibodies in the clinic (37, 38). To investigate the role of Fc effector function in the *in vivo* activity of fully human anti–CTLA-4 and to identify the mechanisms controlling the ability of these antibodies to deplete Tregs in tumors, we developed a mouse model humanized for both human CTLA-4 and human FcγRs (humanized CTLA-4/FcγR mice; **Fig. 1A**). In brief, we used human CTLA-4 transgenic mice on a mouse *Ctla4*$^{-/-}$ background (4), and we crossed them to our previously described humanized FcγR mice in which human FcγRs have been inserted as transgenes in place of murine FcγRs that are deleted (26). We found that humanized CTLA-4/FcγR mice are viable, and they breed and develop normally without clinical evidence of any autoimmune phenomenon, suggesting normal function of the CTLA-4 checkpoint. Phenotypic analysis of tumor-infiltrating CD45^{+}CD3^{+} T cells isolated from humanized CTLA-4/FcγR mice confirmed expression of human CTLA-4 in CD8^{+} T cells, FOXP3^{-} conventional CD4^{+} T cells (Tconv) and FOXP3^{+} Tregs (**Fig. 1B** and **C**). In three distinct transplantable tumor models (MC38, B16, and MCA-205), we found that the expression profiles of CTLA-4 were similar when comparing T cells in tumors isolated from WT C57BL/6J (expressing mouse CTLA-4) and humanized CTLA-4/FcγR mice (expressing human CTLA-4), with the exception of tumor-infiltrating CD8^{+} T cells, which expressed more CTLA-4 in humanized CTLA-4/FcγR mice (**Fig. 1C**; Supplementary Fig. S1A and S1B), consistent with findings observed in patients with cancer (8). Other than this, the key expression patterns were conserved, with CTLA-4 expression mainly restricted to CD4^{+}FOXP3^{+} Tregs, and a level of expression higher in tumors as compared with spleen or lymph node (**Fig. 1C**; Supplementary Fig. S1A and S1B). Finally, we confirmed that humanized CTLA-4/FcγR mice expressed the whole set of human FcγRs in both spleens and tumors (**Fig. 1D**), fully validating our humanized mouse model. To leverage this humanized system, we next cloned the variable heavy and light sequences (Fab) of ipilimumab (clone 10D1) and tremelimumab (clone 1121), the two main human anti–CTLA-4 approved for use in the clinic, and expressed them on their respective human IgG1 and IgG2 Fc backbones (**Fig. 1E**). We assessed their binding to human CTLA-4 by surface plasmon resonance (**Fig. 1F**), and we verified their ability to block the interaction between human CTLA-4 and B7.1 by competitive ELISA (**Fig. 1G**).

Human anti–CTLA-4 are limited in their capacity to deplete intratumoral Tregs in humanized CTLA-4/FcγR mice

To evaluate the contributions of the Fab and Fc domains to the *in vivo* activity of ipilimumab and tremelimumab, we expressed each of them as an IgG1 or IgG2 Fc format, which display moderate or weak binding to FcγRs, respectively (**Fig. 2A**; ref. 15). We then tested their *in vivo* antitumor activity in humanized CTLA-4/FcγR mice bearing MC38 tumors (**Fig. 2B**), a tumor model that is associated with complete response to murine anti–CTLA-4 (6, 39). We identified signs of antitumor activity for both ipilimumab and tremelimumab, although the increased tumor control observed following treatment with ipilimumab was not statistically significant when compared with the control group (**Fig. 2C** and **D**). Ipilimumab and tremelimumab had similar antitumor activity irrespective of their IgG Fc backbone (**Fig. 2C** and **D**), suggesting no major contribution of the Fc effector function to the antitumor activity of these antibodies. Neither the IgG1 nor IgG2 Fc format had antitumor activity in the less-immunogenic B16 tumor model (**Fig. 2E**). Flow cytometric analysis of T cells infiltrating MC38 tumors revealed that only ipilimumab-IgG1 led to a modest decrease of FOXP3^{+} Tregs whereas both ipilimumab-IgG1 and -IgG2 increased the infiltration of CD8^{+} T cells (**Fig. 2F**), suggesting that CD8^{+} T-cell activation, rather than Treg depletion, was responsible for the antitumor activity of recombinant ipilimumab antibodies in humanized CTLA-4/FcγR mice. Ipilimumab-IgG1 and -IgG2 did not modulate any T-cell subset in B16 tumors (**Fig. 2G**), in line with the absence of antitumor effect in this model (**Fig. 2E**). Collectively, these results suggest that ipilimumab and tremelimumab mainly rely on their checkpoint-blocking activity to control tumors in humanized CTLA-4/FcγR mice, and their Fc effector function is not sufficient to provide additional therapeutic benefits, which recapitulates the findings observed in patients (12).

The inhibitory Fc receptor FcγRIIB is highly expressed in the TME

To verify that the poor depletion of intratumoral Tregs observed during treatment with ipilimumab was not due to target-specific factors, we examined the depleting capabilities of a murine anti-CD4

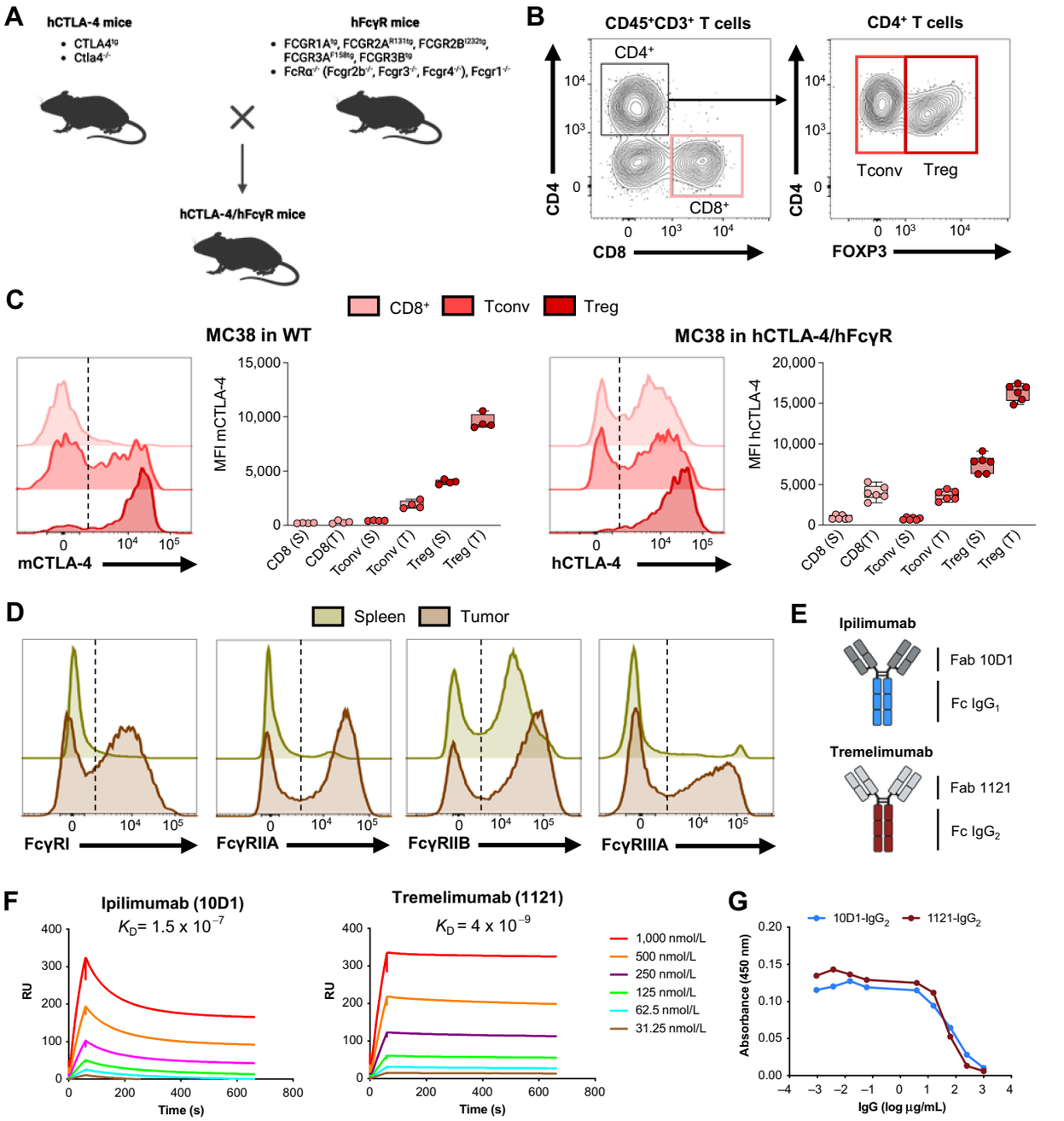

Figure 1.

A humanized mouse model to study the Fc effector function of human anti–CTLA-4. **A,** Schematic drawing describing the generation of humanized CTLA-4/FcγR mice. The genotypes of the mouse strains used for the crossing are presented. **B** and **C,** Flow cytometric analysis of CTLA-4 in $CD45^+CD3^+$ T cells isolated from spleens and tumors from humanized CTLA-4/FcγR mice. **B,** Representative dot plots illustrating the gating strategy for identification of $CD8^+$ T cells, $FOXP3^-$ conventional $CD4^+$ T cells (Tconv) and $FOXP3^+$ $CD4^+$ Tregs in MC38 tumors from humanized CTLA-4/FcγR mice. **C,** Levels of expression of mouse CTLA-4 (mCTLA-4) and human CTLA-4 (hCTLA-4) in the indicated T-cell subsets in spleens (S) and tumors (T) from WT (left, $n = 4$) and humanized CTLA-4/FcγR mice (right, $n = 6$) bearing MC38 tumors. Representative histograms and quantification of the mean fluorescence intensity (MFI) ± SEM are shown. Dotted lines indicate Fluorescence Minus One (FMO) controls. Each symbol represents an individual mouse and are from one experiment. **D,** Flow cytometric analysis of human FcγRs in $CD45^+$ immune cells isolated from spleens and tumors from humanized CTLA-4/FcγR mice bearing MC38 tumors. Representative histograms from one experiment are shown. Dotted lines indicate FMO controls. **E,** Schema outlining the composition of the recombinant human anti–CTLA-4 antibodies used in the study. The Fab and Fc regions used for the generation of recombinant ipilimumab (top) and tremelimumab (bottom) antibodies are described. **F,** Evaluation of the binding of the recombinant ipilimumab (left) and tremelimumab (right) antibodies to hCTLA-4 by surface plasmon resonance. The dissociation constant (K_D) of each antibody is shown. RU, response units. Data are from one experiment. **G,** Competitive ELISA evaluating the capacity of recombinant hIgG2 ipilimumab (clone 10D1) and hIgG2 tremelimumab (clone 1121) to block the interaction between hCTLA-4 and human B7.1 (CD80). Data indicate means for triplicate wells and are from one experiment. Panels **A** and **E** were created with BioRender.com.

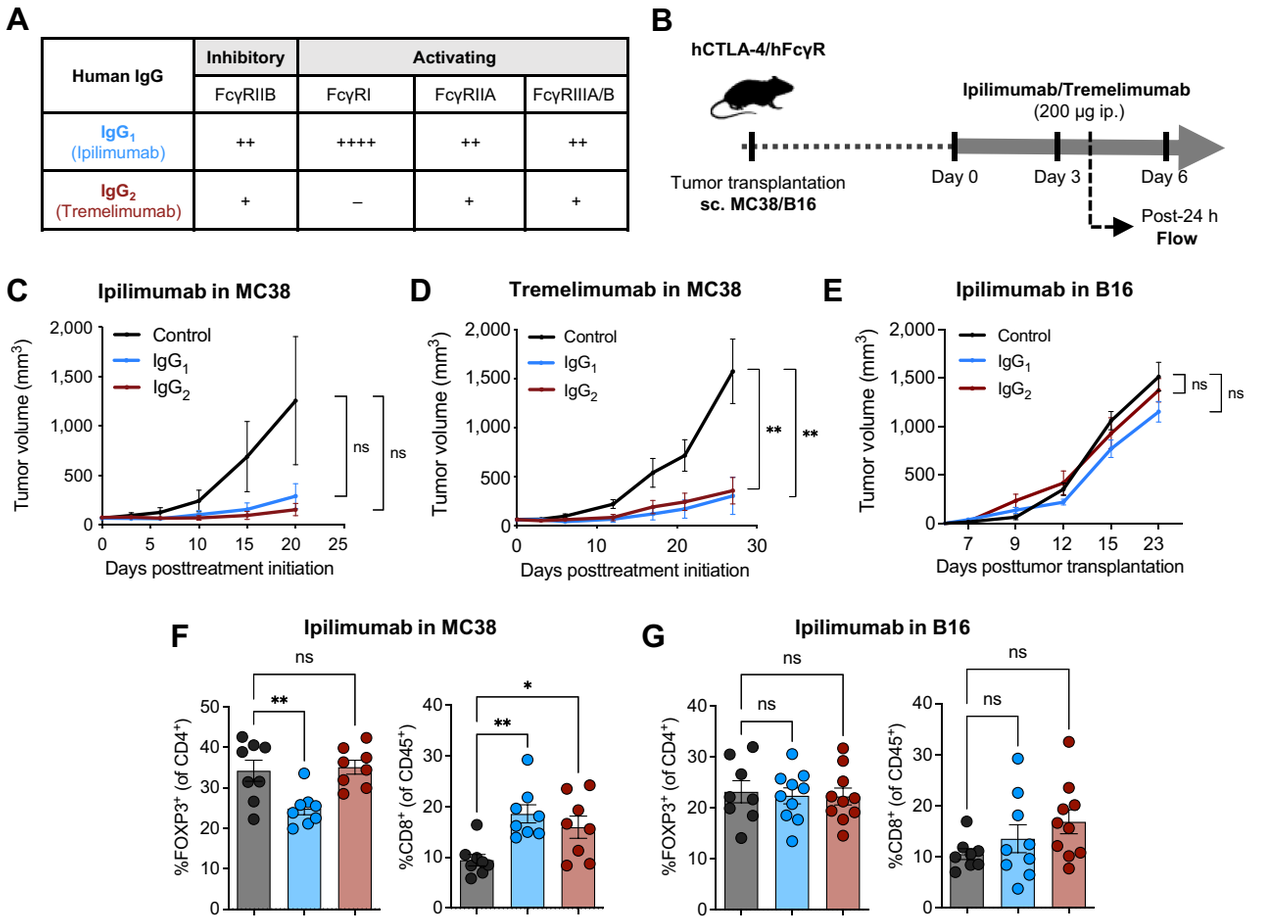

Figure 2.

Human anti–CTLA-4 have limited Treg-depleting and antitumor activities in humanized CTLA-4/FcγR mice. **A,** Binding profiles of human IgG1 (hIgG1) and human IgG2 (hIgG2) to human FcγRs. The relative binding affinities presented were defined on the basis of affinity constants previously assessed by surface plasmon resonance (34). **B,** Schema of experimental design indicating the treatment timing and dosage of human anti–CTLA-4 in humanized CTLA-4/FcγR mice. Average growth ± SEM of MC38 tumors in humanized CTLA-4/FcγR mice treated with ipilimumab (**C**) or tremelimumab (**D**). Each antibody was evaluated with both a hIgG1 or a hIgG2 Fc backbone and compared with hIgG1 isotype control ($n = 5$–10 mice/group, two independent experiments). **E,** Average growth ± SEM of B16 tumors in humanized CTLA-4/FcγR mice treated with ipilimumab. The antibody was evaluated with both a hIgG1 or a hIgG2 Fc backbone and compared with hIgG1 isotype control ($n = 5$ mice/group, one experiment). In each experiment (**C–E**), *P* values were determined at last timepoint of tumor assessment by one-way ANOVA with Tukey multiple comparison test. Flow cytometry analysis of FOXP3$^+$ Tregs and CD8$^+$ T cells in MC38 (**F**) and B16 (**G**) tumors from humanized CTLA-4/FcγR mice treated with recombinant hIgG1 or hIgG2 ipilimumab. A hIgG1 isotype control antibody was used for the control group. Data indicate means ± SEM and each symbol represents an individual mouse ($n = 8$–10 mice/group, two independent experiments). *P* values were determined by one-way ANOVA with Tukey multiple comparison test. *, $P < 0.05$; **, $P < 0.01$; ns, not significant.

(clone GK1.5) bearing a human IgG1 Fc backbone, similarly to the composition of ipilimumab-IgG1. In humanized FcγR mice bearing MC38 tumors (Supplementary Fig. S2A), we detected a small reduction of CD4$^+$ T cells in peripheral blood following treatment with GK1.5-IgG$_1$ (Supplementary Fig. S2B). However, we did not observe any reduction of tumor-infiltrating CD4$^+$ T cells (Supplementary Fig. S2C), indicating that lack of effective antibody-mediated cell depletion was not target dependent, but rather a feature of the TME.

The ability of effector immune cells to deplete IgG-coated cells depends on the IgG subclass of the antibody and its binding affinities for FcγRs and on the balance between the expression of activating FcγRs and the inhibitory FcγRIIB on the surface of the effector cells (15, 17). A role for activating FcγRs in the antitumor activity of ipilimumab, in particular FcγRIIIA, has been described in patients with metastatic cancer (8, 40, 41). However, the role of the inhibitory FcγRIIB in this context has been less explored. By flow cytometric analysis, we found that the activating FcγRIIIA was indeed expressed by a subset of tumor-infiltrating immune cells in humanized CTLA-4/FcγR mice (**Fig. 3A**). Furthermore, we found that FcγRIIB was also expressed by a substantial portion of tumor-infiltrating immune cells (**Fig. 3A**), and the percentage of cells expressing FcγRIIB exceeded the percentage of cells expressing FcγRIIIA in MC38, MCA-205, and B16 tumors (**Fig. 3A–C**), revealing a prevalence for the inhibitory FcγRIIB in the TME. To further define the role of FcγRIIB expression in the TME, we compared the mean fluorescence intensity (MFI) of FcγRIIB in matched tumors and peripheral organs (**Fig. 3D**), and we found that the level of expression was consistently higher in tumors across the

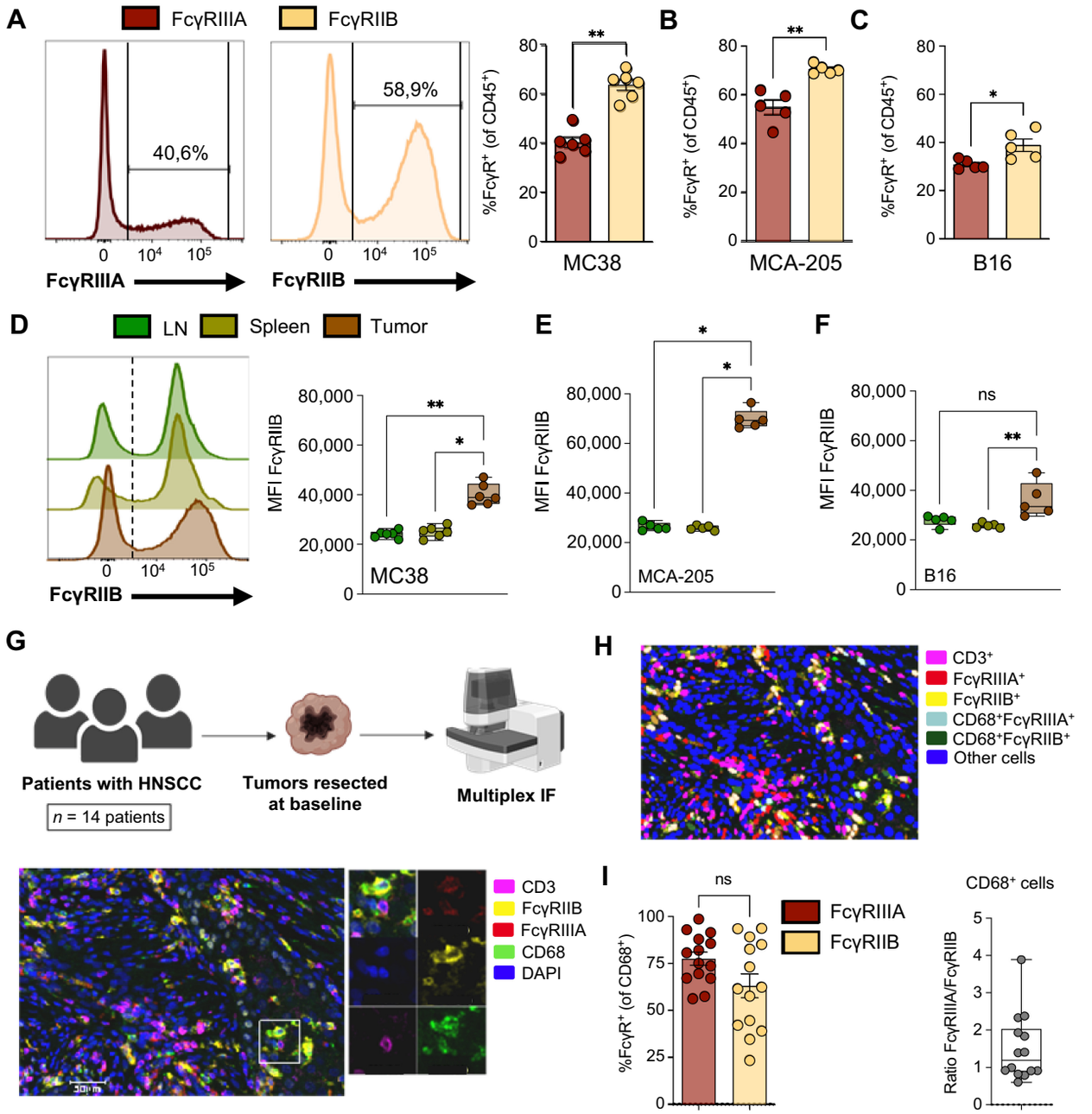

Figure 3.

The inhibitory Fc receptor FcγRIIB is highly expressed in the TME. **A–F,** Flow cytometric analysis of human FcγRs in tumors and lymphoid organs from humanized CTLA-4/FcγR mice. Percentages of expression of the activating FcγRIIIA and the inhibitory FcγRIIB in CD45$^+$ immune cells from MC38 (**A**), MCA-205 (**B**), and B16 (**C**) tumors. Representative histograms and quantification of the mean percentage ± SEM of cells expressing the indicated FcγR are shown. Each symbol represents an individual mouse and data are from one experiment ($n = 5$–6 mice/model). *P* values were determined by Mann–Whitney test. Expression levels of the inhibitory FcγRIIB in CD45$^+$ immune cells isolated from tumor-draining lymph nodes, spleens, and tumors from mice bearing MC38 (**D**), MCA-205 (**E**), or B16 (**F**) tumors. Representative histograms and quantification of the MFI ± SEM of FcγRIIB in CD45$^+$FcγRIIB$^+$ cells are shown. Dotted lines indicate Fluorescence Minus One (FMO) control. Each symbol represents an individual mouse and data are from one experiment ($n = 5$–6 mice/model). *P* values were determined by Kruskal–Wallis test with Dunn multiple comparison test. **G–I**, mIF analysis of human FcγRs in human tumors. **G,** Schematic drawing indicating the cohort of patients and experimental procedure. Resected tumors from patients ($n = 14$) with HNSCC were analyzed by mIF for CD3, CD68, FcγRIIB, FcγRIIIA, and DAPI (top). Representative image (of 14 samples) showing myeloid cells (CD68, green) expressing FcγRIIB (yellow) and/or FcγRIIIA (red) in a tumor resected from a patient (bottom). Inset shows a higher magnification image of the boxed area with all individual stainings. **H,** Representative segmentation mask obtained from the original image shown in **G** and the distinct cell phenotypes analyzed in the study. **I,** Quantification of the percentage of cells expressing the indicated FcγR in CD68$^+$ myeloid cells (left). Each symbol represents a patient and data indicate means ± SEM. The ratio of FcγRIIIA$^+$ to FcγRIIB$^+$ cells among CD68$^+$ myeloid cells is indicated (right). *P* value was determined by Mann–Whitney test. *, $P < 0.05$; **, $P < 0.01$; ns, not significant. Panel **G** was created with BioRender.com.

three models (**Fig. 3D–F**), suggesting upregulation of FcγRIIB in the TME.

To validate our findings in a human setting, we used mIF to characterize the expression of the activating FcγRIIIA and the inhibitory FcγRIIB in baseline tumor specimens from patients with head and neck squamous cell carcinoma (HNSCC; **Fig. 3G**; Supplementary Table S3). We found that FcγRIIIA and FcγRIIB were expressed in all tested tumors ($n = 14$ patients), indicating that expression of FcγRIIB in tumor was not specific to murine models. FcγRs were mainly expressed by $CD68^+$ myeloid cells, while their expression by $CD3^+$ T cells was very rare (**Fig. 3G**). Our quantitative analyses revealed that intratumoral $CD68^+$ myeloid cells similarly expressed FcγRIIIA and FcγRIIB (**Fig. 3H** and **I**), with more than 60% of cells expressing the inhibitory FcγRIIB. Overall, our results indicate that FcγRIIB is highly expressed in the TME in both humanized mice and humans, and could play a role in limiting IgG Fc-dependent responses in tumors.

Limiting FcγRIIB engagement improves the Treg-depleting potency of human anti–CTLA-4

We hypothesized that FcγRIIB is a checkpoint limiting the Fc-dependent activity of IgG antibodies in tumors, and that interfering with its binding and activity could increase the capacity of human anti–CTLA-4 to deplete Tregs in tumors. To test this hypothesis, we employed two complementary strategies: (i) Administration of a blocking anti-human FcγRIIB (clone 2B6; ref. 27) in combination with ipilimumab; and (ii) Fc engineering to compare anti–CTLA-4 with distinct binding affinities for activating FcγRs and the inhibitory FcγRIIB (**Fig. 4A**). In brief, we generated antibodies incapable of interacting with FcγRs (Fc null N297A or GRLR; refs. 30, 42), afucosylated antibodies, which had increased binding for the activating FcγRIIIA while retaining similar binding to FcγRIIB (Supplementary Fig. S3A; ref. 30), and GAALIE Fc-engineered antibodies, which have increased binding for activating FcγRs and reduced binding for the inhibitory FcγRIIB (29, 30). When testing these various treatment conditions in the MC38 tumor model (**Fig. 4B**), we found that blocking FcγRIIB significantly increased the capacity of ipilimumab to deplete Tregs in tumors (**Fig. 4C**), indicating that FcγRIIB is functional in the TME, and limits the Fc effector function of ipilimumab. In addition, both ipilimumab-afucosylated and ipilimumab-GAALIE signicantly reduced Tregs in tumors, while ipilimumab-Fc null did not have any impact (**Fig. 4C**), showing that favoring ipilimumab interactions with activating FcγRs through Fc engineering can overcome FcγRIIB inhibition. In addition, directly limiting binding to FcγRIIB, either via antibody blocking or via Fc engineering using the GAALIE Fc variant, significantly enhanced the antitumor activity of ipilimumab in the MC38 model (**Fig. 4D**). There was also a trend for increased tumor control with ipilimumab-afucosylated (**Fig. 4D**), but this effect did not reach statistical significance in our grouped analysis, showing that ipilimumab-GAALIE was more effective in the MC38 tumor model. This improved efficacy was further demonstrated by an increased percentage of mice showing complete response to treatment (Supplementary Fig. S3B and S3C), with a 100% response rate in the combined ipilimumab and anti-FcγRIIB group.

On the basis of our results, we propose that FcγRIIB blocking represents a promising avenue to increase the Fc effector function of human anti–CTLA-4 in patients. However, administering a systemic FcγRIIB-blocking antibody may not be feasible due to the presence of FcγRIIB on circulating immune cells, and the potential side effects triggered by FcγRIIB-expressing B cells, which could lead to IgG-mediated inflammation and toxicity (15). Therefore, we focused our subsequent studies on the Fc-engineered ipilimumab-GAALIE and evaluated its efficacy in two other models (**Fig. 4B**). Ipilimumab-GAALIE significantly improved the control of tumors in the MB49 model (**Fig. 4E**), and also in the B16 model (**Fig. 4F**), which we previously identified as insensitive to original ipilimumab (**Fig. 2E**). In addition, we found that blocking FcγRIIB in combination with ipilimumab-GAALIE could not further improve antitumor efficacy in the B16 tumor model (Supplementary Fig. S3D and S3E), suggesting that antibody binding to FcγRIIB is optimally reduced with the GAALIE Fc variant. Finally, we found that tremelimumab-GAALIE also had robust antitumor efficacy in the MC38 tumor model (**Fig. 4G**), confirming the potency of the GAALIE Fc variant with a second human anti–CTLA-4. Overall, our results indicate that FcγRIIB represents a checkpoint limiting the ability of human anti–CTLA-4 to deplete Tregs in tumors, and that optimizing the Fc domain of human anti–CTLA-4 can overcome this limitation.

Potent depletion of tumor-infiltrating Tregs with Fc-engineered anti-CCR8

While CTLA-4 is upregulated on Tregs, it is also expressed on non-Treg subsets, both on their cell surface and in intracellular stores that can be mobilized following T-cell activation (4). Blockade of CTLA-4 on effector T cells is thought to be a primary driver of immune-related adverse events (irAE) that occur in a substantial proportion of patients receiving anti–CTLA-4 immunotherapy (1). Antibody-based targeting of other Treg-associated markers such as CC motif chemokine receptor 4 (CCR4) and CD25 have been investigated in patients (43), but these approaches have shown limited clinical benefit, which is also due to the expression of CCR4 and CD25 on non-Treg immune cell populations. In contrast, CC motif chemokine receptor 8 (CCR8) has been recently identified as a specific marker of tumor-infiltrating Tregs (44, 45), with minimal expression on tumor-infiltrating effector $CD4^+$ and $CD8^+$ T cells, and peripheral Tregs. As a result, CCR8-targeting antibodies represent an exciting approach to selectively deplete Tregs in the TME (46–48).

To determine how Treg depletion by anti-CCR8 could be optimized, we generated chimeric antibodies composed of a murine anti-CCR8 Fab (clone SA214G2) and various human IgG1 Fc domains with distinct binding profiles to FcγRs: intact Fc, Fc null GRLR, afucosylated Fc and GAALIE Fc. We confirmed that CCR8 was mainly expressed by tumor-infiltrating Tregs in humanized FcγR mice (Supplementary Fig. S4A), and assessed the antitumor activity of the different anti-CCR8 in the MC38 tumor model (**Fig. 5A**). While both SA214G2-afucosylated and SA214G2-GAALIE elicited antitumor activity in this model (Supplementary Fig. S4B and S4C), only SA214G2-GAALIE showed a significant improvement of tumor control when compared with the control group (**Fig. 5B**). In contrast, SA214G2-IgG_1 or SA214G2-Fc null had no antitumor activity (**Fig. 5B**). Flow cytometric analysis of tumors confirmed a potent depletion of Tregs following treatment with SA214G2-GAALIE (**Fig. 5C**). Interestingly, we noticed that SA214G2-IgG1 was able to slightly reduce Tregs in tumors (**Fig. 5C**), similarly to ipilimumab-IgG1 (**Fig. 2F**), but this was not sufficient enough to drive antitumor activity (**Fig. 5B**; Supplementary Fig. S4B and S4C), highlighting the importance of optimizing the FcγR binding profile of anti-CCR8 for maximal depletion of Tregs in the TME. We confirmed these findings in the MB49 tumor model (**Fig. 5D** and **E**), and we also observed single-agent activity of SA214G2-GAALIE in the aggressive B16 tumor model (**Fig. 5F**). We concluded that increasing the binding of anti-CCR8 to activating FcγRs (i.e., afucosylated antibodies) is sufficient to drive *in vivo* activity, but further decreasing their binding to FcγRIIB (i.e., Fc-engineered GAALIE antibodies) is required for maximal efficacy, showing that

A

Human IgG_1 Fc variant	Inhibitory	Activating		
	FcγRIIB	FcγRI	FcγRIIA	FcγRIIIA/B
WT	++	++++	++	++
N297A/GRLR	–	–	–	–
Afucosylated	++	++++	++	+++++
GAALIE	+	++++	+++++	+++++

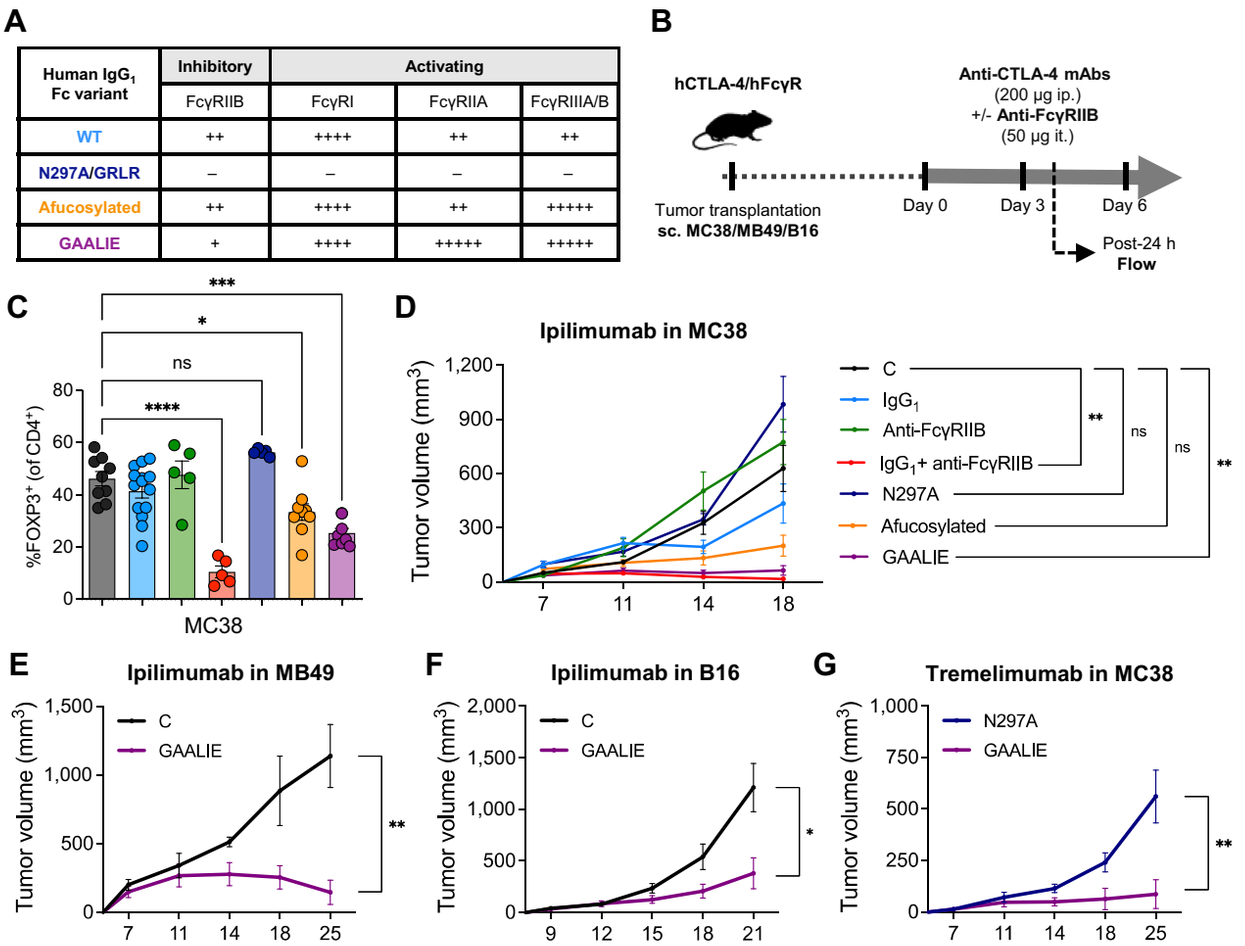

Figure 4.

Limiting the binding of human anti–CTLA-4 to FcγRIIB improves Treg depletion and tumor control. **A,** Schema of experimental design indicating the treatment timing and dosage of human IgG1 (hIgG1) ipilimumab alone or in combination with a human FcγRIIB–blocking antibody (clone 2B6), as well as various Fc-engineered hIgG1 anti–CTLA-4 (ipilimumab or tremelimumab). **B,** Binding profiles of distinct $hIgG_1$ Fc variants to human FcγRs. The relative binding affinities presented were defined based on affinity constants previously assessed by surface plasmon resonance (29, 30). **C,** Flow cytometry analysis of $FOXP3^+$ Tregs in MC38 tumors from humanized CTLA-4/FcγR mice treated with indicated treatments (color legend in **D**). A hIgG1 isotype control antibody was used for the control group. Data indicate means ± SEM and each symbol represents an individual mouse ($n = 5$–14 mice/group, three independent experiments). *P* values were determined by one-way ANOVA with Tukey multiple comparison test. **D,** Average growth ± SEM of MC38 tumors in humanized CTLA-4/FcγR mice treated with indicated treatments ($n = 5$–20 mice/group, four independent experiments). A hIgG1 isotype control antibody was used for the control group. *P* values were determined at last timepoint of tumor assessment by one-way ANOVA with Tukey multiple comparison test. Average growth ± SEM of MB49 (**E**), B16 (**F**), and MC38 (**G**) tumors in humanized CTLA-4/FcγR mice treated with Fc-engineered hIgG1 GAALIE ipilimumab (**E** and **F**) or Fc-engineered hIgG1 GAALIE tremelimumab (**G**; $n = 4$–6 mice/group, one experiment). A hIgG1 isotype control antibody (**E** and **F**) or Fc null hIgG1 (N297A) tremelimumab (**G**) were used for the control groups. *P* values were determined at last timepoint of tumor assessment by Mann–Whitney test. *, $P < 0.05$; **, $P < 0.01$; ***, $P < 0.001$; ****, $P < 0.0001$; ns, not significant.

FcγRIIB limits the Fc effector function of various therapeutic antibodies in the TME.

Discussion

The FDA approvals of antibodies blocking the inhibitory checkpoints PD-1 and CTLA-4 on T cells have offered new hope for patients with cancer, leading to profound and durable responses in a subset of them. However, despite these encouraging advances, our understanding of how these agents actually target and modulate immune cells in humans remains incomplete. Prior preclinical studies have demonstrated that Fc-dependent depletion of tumor-infiltrating Tregs contributes to the efficacy of anti–CTLA-4 immunotherapy (5–11). This mechanism relies on engagement of the activating FcγRIV on intratumoral myeloid cells that subsequently induce ADCP/ADCC (5). In patients, initial studies reported that ipilimumab could induce the depletion of Tregs by $CD14^+FcγRIIIA^+$ monocytes *ex vivo* (40), and more recent studies have revealed that patients expressing the $FcγRIIIA^{158V}$ variant, which has increased binding affinity to human IgG1 (8), or patients having tumor enriched in FcγRIIIA-expressing macrophages (41), have improved response to ipilimumab, suggesting that Fc-dependent mechanisms could potentially improve the

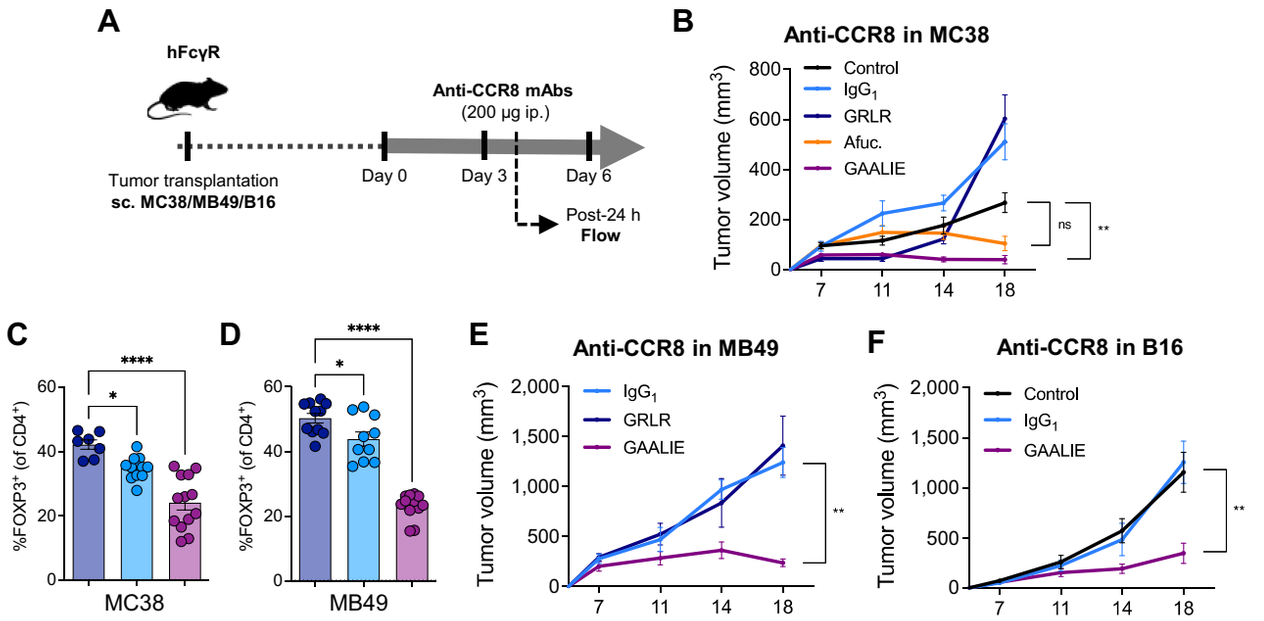

Figure 5.

Targeting tumor-infiltrating Tregs with Fc-engineered anti-CCR8 induces potent antitumor activity. **A,** Schema of experimental design indicating the treatment timing and dosage of a human IgG1 (hIgG1) anti-murine CCR8 (clone SA214G2), as well as various Fc-engineered hIgG1 versions of this same antibody. **B,** Average growth ± SEM of MC38 tumors in humanized FcγR mice treated with indicated treatments ($n = 4$–17 mice/group, three independent experiments). A hIgG1 isotype control antibody was used for the control group. *P* values were determined at last time point of tumor assessment by one-way ANOVA with Tukey multiple comparison test. **C** and **D,** Flow cytometry analysis of FOXP3$^+$ Tregs in MC38 tumors from humanized FcγR mice treated with indicated treatments (color legend in **B**). Fc null hIgG1 (GRLR) anti-murine CCR8 were used for the control groups. Data indicate means ± SEM and each symbol represents an individual mouse ($n = 7$–13 mice/group, two independent experiments). *P* values were determined by one-way ANOVA with Tukey multiple comparison test. Average growth ± SEM of MB49 (**E**) and B16 (**F**) tumors in humanized FcγR mice treated with indicated treatments ($n = 4$–11 mice/group, one experiment in **E** and two independent experiments in **F**). Fc null hIgG1 (GRLR) anti-murine CCR8 (**E**) or a human IgG1 isotype control antibody (**F**) were used for the control groups. *P* values were determined at last timepoint of tumor assessment by one-way ANOVA with Tukey multiple comparison test. *, $P < 0.05$; **, $P < 0.01$; ****, $P < 0.0001$; ns, not significant.

antitumor activity of ipilimumab in some settings. However, ipilimumab, just like tremelimumab, is not able to deplete tumor-infiltrating Tregs in the vast majority of patients (12), and the mechanisms behind this observation remained unclear. Here, we developed a mouse model humanized for CTLA-4 and FcγRs to elucidate the contribution of the Fc domain to the *in vivo* activity of human anti–CTLA-4. Similar to what has been observed in patients, we found that human anti–CTLA-4 poorly deplete intratumoral Tregs in humanized CTLA-4/FcγR mice, and this is associated with modest antitumor activity. This limitation appears to be due to the inhibitory Fc receptor FcγRIIB, which is abundantly expressed in the TME. Blocking FcγRIIB or engineering anti–CTLA-4 to have decreased binding to FcγRIIB, rescues Treg depletion and unleashes antitumor efficacy. These findings were further validated with antibodies targeting CCR8, a chemokine receptor selectively expressed on tumor-infiltrating Tregs. Collectively, these studies identify FcγRIIB as an important immune checkpoint in the TME and suggest Fc engineering as an effective strategy to overcome this limitation.

Central to the mechanism of FcγR-mediated depletion of IgG-coated cells is the observation that engagement of activating FcγRs (generally FcγRIIIA in humans and FcγRIV in mice) is balanced by engagement of the inhibitory FcγRIIB, setting a threshold for effector-cell activation (15, 17, 18). Therefore, the ability of an IgG antibody to induce ADCC/ADCP is highly influenced by its binding affinities to the distinct FcγRs. For instance, murine IgG2a displays a very high affinity for the activating murine FcγRIV while it has a relatively weak interaction for the inhibitory murine FcγRIIB (17), resulting in an extremely high activating to inhibitory (A/I) ratio. In contrast, human IgG1 displays a significantly lower A/I ratio for human FcγRs, which may explain in part the differences observed in the capacity of murine IgG2a anti–CTLA-4 and human IgG1 anti–CTLA-4 to deplete tumor-infiltrating Tregs (6, 12). Moreover, the Fc effector function of IgG antibodies is governed by the level of expression of FcγRs on immune effector cells, and tissue-intrinsic factors can modulate the expression of FcγRs (15). We revealed that the expression of the inhibitory FcγRIIB is particularly increased within the TME, where it acts as a checkpoint limiting the Fc effector function of IgG antibodies. These findings are important because most attemps to increase the Fc effector function of human anti–CTLA-4 have focused on enhancing their engagement to the activating FcγRIIIA through either afucosylation of the antibody (e.g., BMS-986218, an afucosylated form of ipilimumab; NCT03110107) or Fc engineering (e.g., AGEN1181, a human anti–CTLA-4 bearing the human IgG1 Fc variant SDALIE; NCT03860272). While our results indicate that increasing the binding of human anti–CTLA-4 to FcγRIIIA enhances intratumoral Treg depletion and antitumor activity, they also show that limiting the binding to FcγRIIB is required to optimally improve antitumor activity. Finally, although we did not specifically interrogate the role of FcγRIIA in our experiments, previous reports indicate that it could be involved in antibody-mediated cell depletion in other tumor settings (8, 29), suggesting that FcγRIIA could also contribute to the activity of Treg-targeting antibodies. Therefore, the human IgG1 Fc variant GAALIE appears to be

an attractive therapeutic tool as it uniquely combines increased affinities for the activating FcγRIIA/IIIA and reduced affinity for FcγRIIB.

Anti–CTLA-4 were the first immune checkpoint inhibitors approved for the treatment of cancer and have revolutionized our approach to cancer therapy as a field. However, their utilization in patients is challenged by toxicities beause of the central role of CTLA-4 in immune tolerance and the expression of CTLA-4 on peripheral T-cell populations (1, 3). Although irAEs induced by anti–CTLA-4 may essentially result from their checkpoint-blocking activity (49), these toxicity issues suggest that CTLA-4 might not be the ideal target for the effective translation of Treg-depleting strategies into the clinic. Thus, many groups are working to define alternative Treg-associated targets, among which, CCR8 has been identified as a specific marker of tumor-infiltrating Tregs (44, 45). We demonstrated that Fc-engineered anti-CCR8 can overcome the FcγRIIB checkpoint in the TME and lead to robust antitumor activity in multiple tumor models. These results support the clinical evaluation of Fc-engineered anti-CCR8 in patients, and indicate that limiting their binding to FcγRIIB is required to maximize their efficacy.

In conclusion, our findings demonstrate FcγRIIB as an immune checkpoint limiting the Fc effector function of IgG antibodies in the TME, and inform Fc engineering strategies to overcome this limitation and improve the efficacy of Treg-targeting antibodies in patients.

Authors' Disclosures

D.A. Knorr reports other support from Regeneron Pharmaceuticals outside the submitted work. R.S. Leidner reports grants from Bristol Myers Squibb during the conduct of the study, grants from Incyte, personal fees from CDR-Life, Vir and Merck, and nonfinancial support from Celldex, Clinigen, and Ubivac outside the submitted work. S.M. Jensen reports grants from Bristol Myers Squibb and Akoya Biosciences during the conduct of the study. R.B. Bell reports grants from BMS during the conduct of the study. C.B. Bifulco reports personal fees from Roche, Sanofi, Agilent, and Incendia outside the submitted work. B. Piening reports grants and personal fees from Eli Lilly and Company and grants from Illumina outside the submitted work. B.A. Fox reports grants from Bristol Myers Squibb and Akoya Biosciences during the conduct of the study, grants from Incyte and Macrogenomics, personal fees from UbiVac, Turnstone, and Pfizer, and personal fees from Neogenomics, Calidi, PrimeVax, and Hookipa outside the submitted work. J.V. Ravetch reports grants from NIH, National Center for Advancing Translational Sciences, and National Cancer Institute during the conduct of the study; in addition, J.V. Ravetch has a patent for WO2019125846A1 issued. No disclosures were reported by the other authors.

Authors' Contributions

D.A. Knorr: Conceptualization, resources, data curation, formal analysis, supervision, funding acquisition, validation, investigation, visualization, methodology, writing–original draft, project administration, writing–review and editing. **L. Blanchard:** Conceptualization, data curation, formal analysis, validation, investigation, visualization, methodology, writing–review and editing. **R.S. Leidner:** Resources, formal analysis, supervision, funding acquisition, investigation, writing–original draft, project administration, writing–review and editing. **S.M. Jensen:** Data curation, formal analysis, validation, investigation, visualization, methodology. **R. Meng:** Data curation, formal analysis, validation, investigation. **A. Jones:** Validation, investigation. **C. Ballesteros-Merino:** Data curation, formal analysis, supervision, validation, investigation. **R.B. Bell:** Resources, data curation, supervision, funding acquisition. **M. Baez:** Formal analysis, validation, investigation. **A. Marino:** Investigation, methodology. **D. Sprott:** Formal analysis, investigation. **C.B. Bifulco:** Formal analysis, supervision, visualization. **B. Piening:** Formal analysis, supervision, funding acquisition, project administration. **R. Dahan:** Data curation, formal analysis, investigation. **J.C. Osorio:** Conceptualization, data curation, formal analysis, supervision, validation, investigation, visualization, writing–review and editing. **B.A. Fox:** Resources, supervision, funding acquisition, visualization. **J.V. Ravetch:** Resources, supervision, funding acquisition, writing–original draft, project administration, writing–review and editing.

Acknowledgments

The authors would like to thank P. Smith, B. Bhagwandin-Colisi, A. Martin Mozqueda, E. Lam, and R. Peraza for maintaining the humanized mouse strains, and all the members of the J.V. Ravetch laboratory for excellent technical assistance and helpful feedback. This work was supported by following grants from the National Institutes of Health (NIH): UL1TR001866 and KL2TR001865 from the National Center for Advancing Translational Sciences NIH Clinical and Translational Science Award Program (D.A. Knorr), K08CA248966 (D.A. Knorr), R35CA196620, R01CA244327, and P01CA190174 (J.V. Ravetch), MSK Specialized Program of Research Excellence in Bladder Cancer P50CA221745 through a Developmental Research Program Award, and the NCI Cancer Center Support Grant P30CA008748. The content is solely the responsibility of the authors and does not necessarily represent the official views of the NIH. C. Ballesteros-Merino, S.M. Jensen, R.S. Leidner, and B.A. Fox would like to thank the Harder Family, Robert W. Franz, Elsie Franz Finley, the Murdock Trust, the Chiles Foundation, and Nancy Lematta. R.S. Leidner is also supported by Bristol Myers Squibb IO-ON.

Note

Supplementary data for this article are available at Cancer Immunology Research Online (http://cancerimmunolres.aacrjournals.org/).

Received May 21, 2023; revised October 10, 2023; accepted December 21, 2023; published first December 26, 2023.

References

1. Morad G, Helmink BA, Sharma P, Wargo JA. Hallmarks of response, resistance, and toxicity to immune checkpoint blockade. Cell 2021;184:5309–37.
2. Sharma P, Allison JP. Dissecting the mechanisms of immune checkpoint therapy. Nat Rev Immunol 2020;20:75–6.
3. Wei SC, Duffy CR, Allison JP. Fundamental mechanisms of immune checkpoint blockade therapy. Cancer Discov 2018;8:1069–86.
4. Peggs KS, Quezada SA, Chambers CA, Korman AJ, Allison JP. Blockade of CTLA-4 on both effector and regulatory T cell compartments contributes to the antitumor activity of anti-CTLA-4 antibodies. J Exp Med 2009;206:1717–25.
5. Simpson TR, Li F, Montalvo-Ortiz W, Sepulveda MA, Bergerhoff K, Arce F, et al. Fc-dependent depletion of tumor-infiltrating regulatory T cells co-defines the efficacy of anti-CTLA-4 therapy against melanoma. J Exp Med 2013;210:1695–710.
6. Selby MJ, Engelhardt JJ, Quigley M, Henning KA, Chen T, Srinivasan M, et al. Anti-CTLA-4 antibodies of IgG2a isotype enhance antitumor activity through reduction of intratumoral regulatory T cells. Cancer Immunol Res 2013;1:32–42.
7. Bulliard Y, Jolicoeur R, Windman M, Rue SM, Ettenberg S, Knee DA, et al. Activating Fc γ receptors contribute to the antitumor activities of immunoregulatory receptor-targeting antibodies. J Exp Med 2013;210:1685–93.
8. Vargas FA, Furness AJS, Litchfield K, Joshi K, Rosenthal R, Ghorani E, et al. Fc effector function contributes to the activity of human anti-CTLA-4 antibodies. Cancer Cell 2018;33:649–63.
9. Ingram JR, Blomberg OS, Rashidian M, Ali L, Garforth S, Fedorov E, et al. Anti-CTLA-4 therapy requires an Fc domain for efficacy. Proc Natl Acad Sci U S A 2018;115:3912–7.
10. Ha D, Tanaka A, Kibayashi T, Tanemura A, Sugiyama D, Wing JB, et al. Differential control of human Treg and effector T cells in tumor immunity by Fc-engineered anti-CTLA-4 antibody. Proc Natl Acad Sci U S A 2019;116:609–18.
11. Lax BM, Palmeri JR, Lutz EA, Sheen A, Stinson JA, Duhamel L, et al. Both intratumoral regulatory T cell depletion and CTLA-4 antagonism are required for maximum efficacy of anti-CTLA-4 antibodies. Proc Natl Acad Sci U S A 2023;120:e2300895120.

12. Sharma A, Subudhi SK, Blando J, Scutti J, Vence L, Wargo J, et al. Anti-CTLA-4 immunotherapy does not deplete FOXP3 + regulatory T cells (Tregs) in human cancers. Clin Cancer Res 2019;25:1233–8.
13. Waight JD, Chand D, Dietrich S, Gombos R, Horn T, Gonzalez AM, et al. Selective FcγR Co-engagement on APCs modulates the activity of therapeutic antibodies targeting T cell antigens. Cancer Cell 2018;33:1033–47.
14. Yofe I, Landsberger T, Yalin A, Solomon I, Costoya C, Demane DF, et al. Anti-CTLA-4 antibodies drive myeloid activation and reprogram the tumor microenvironment through FcγR engagement and type I interferon signaling. Nat Cancer 2022;3:1336–50.
15. Nimmerjahn F, Ravetch JV. Fcgamma receptors as regulators of immune responses. Nat Rev Immunol 2008;8:34–47.
16. Bournazos S, DiLillo DJ, Ravetch JV. humanized mice to study FcγR function. Curr Top Microbiol Immunol 2014;382:237–48.
17. Nimmerjahn F, Ravetch JV. Divergent immunoglobulin g subclass activity through selective Fc receptor binding. Science 2005;310:1510–2.
18. Clynes RA, Towers TL, Presta LG, Ravetch JV. Inhibitory Fc receptors modulate in vivo cytotoxicity against tumor targets. Nat Med 2000;6:443–6.
19. Roghanian A, Teige I, Mårtensson L, Cox KL, Kovacek M, Ljungars A, et al. Antagonistic human FcγRIIB (CD32B) antibodies have anti-tumor activity and overcome resistance to antibody therapy *in vivo*. Cancer Cell 2015;27:473–88.
20. Simpson AP, Roghanian A, Oldham RJ, Chan HTC, Penfold CA, Kim HJ, et al. FcγRIIB controls antibody-mediated target cell depletion by ITIM-independent mechanisms. Cell Rep 2022;40:111099.
21. Anthony RM, Kobayashi T, Wermeling F, Ravetch JV. Intravenous gammaglobulin suppresses inflammation through a novel T(H)2 pathway. Nature 2011;475:110–3.
22. Hussain K, Liu R, Smith RCG, Müller KTJ, Ghorbani M, Macari S, et al. HIF activation enhances FcγRIIb expression on mononuclear phagocytes impeding tumor targeting antibody immunotherapy. J Exp Clin Cancer Res 2022;41:131.
23. Todaro M, Alea MP, Di Stefano AB, Cammareri P, Vermeulen L, Iovino F, et al. Colon cancer stem cells dictate tumor growth and resist cell death by production of interleukin-4. Cell Stem Cell 2007;1:389–402.
24. Li Z, Jiang J, Wang Z, Zhang J, Xiao M, Wang C, et al. Endogenous interleukin-4 promotes tumor development by increasing tumor cell resistance to apoptosis. Cancer Res 2008;68:8687–94.
25. Masoud GN, Li W. HIF-1α pathway: role, regulation and intervention for cancer therapy. Acta Pharm Sin B 2015;5:378.
26. Smith P, DiLillo DJ, Bournazos S, Li F, Ravetch JV. Mouse model recapitulating human Fcγ receptor structural and functional diversity. Proc Natl Acad Sci U S A 2012;109:6181–6.
27. Dhodapkar KM, Kaufman JL, Ehlers M, Banerjee DK, Bonvini E, Koenig S, et al. Selective blockade of inhibitory Fcgamma receptor enables human dendritic cell maturation with IL-12p70 production and immunity to antibody-coated tumor cells. Proc Natl Acad Sci U S A 2005;102:2910–5.
28. Kao KS, Gupta A, Zong G, Li C, Kerschbaumer I, Borghi S, et al. Synthetic nanobodies as tools to distinguish IgG Fc glycoforms. Proc Natl Acad Sci U S A 2022;119:e2212658119.
29. Weitzenfeld P, Bournazos S, Ravetch JV. Antibodies targeting sialyl Lewis A mediate tumor clearance through distinct effector pathways. J Clin Invest 2019;129:3952–62.
30. Bournazos S, Corti D, Virgin HW, Ravetch JV. Fc-optimized antibodies elicit CD8 immunity to viral respiratory infection. Nature 2020;588:485–90.
31. Bulliard Y, Jolicoeur R, Zhang J, Dranoff G, Wilson NS, Brogdon JL. OX40 engagement depletes intratumoral Tregs via activating FcγRs, leading to antitumor efficacy. Immunol Cell Biol 2014;92:475–80.
32. DiLillo DJ, Ravetch JV. Differential Fc-receptor engagement drives an anti-tumor vaccinal effect. Cell 2015;161:1035–45.
33. Dahan R, Sega E, Engelhardt J, Selby M, Korman AJ, Ravetch JV. FcγRs modulate the anti-tumor activity of antibodies targeting the PD-1/PD-L1 axis. Cancer Cell 2015;28:285–95.
34. Dahan R, Barnhart BC, Li F, Yamniuk AP, Korman AJ, Ravetch JV. Therapeutic activity of agonistic, human anti-CD40 monoclonal antibodies requires selective FcγR engagement. Cancer Cell 2016;29:820–31.
35. Buchan SL, Dou L, Remer M, Booth SG, Dunn SN, Lai C, et al. Antibodies to costimulatory receptor 4–1BB enhance anti-tumor immunity via T regulatory cell depletion and promotion of CD8 T cell effector function. Immunity 2018;49:958–70.
36. Saban NC, Yalin A, Landsberger T, Salomon R, Alva A, Feferman T, et al. Fc glycoengineering of a PD-L1 antibody harnesses Fcγ receptors for increased antitumor efficacy. Sci Immunol 2023;8:eadd8005.
37. Dilillo DJ, Ravetch JV. Fc-receptor interactions regulate both cytotoxic and immunomodulatory therapeutic antibody effector functions. Cancer Immunol Res 2015;3:704–13.
38. Bournazos S, Gupta A, Ravetch JV. The role of IgG Fc receptors in antibody-dependent enhancement. Nat Rev Immunol 2020;20:633–43.
39. Wei SC, Levine JH, Cogdill AP, Zhao Y, Anang NAAS, Andrews MC, et al. Distinct cellular mechanisms underlie anti-CTLA-4 and anti-PD-1 checkpoint blockade. Cell 2017;170:1120–33.
40. Romano E, Kusio-Kobialka M, Foukas PG, Baumgaertner P, Meyer C, Ballabeni P, et al. Ipilimumab-dependent cell-mediated cytotoxicity of regulatory T cells *ex vivo* by nonclassical monocytes in melanoma patients. Proc Natl Acad Sci U S A 2015;112:6140–5.
41. Lee H, Ferguson AL, Quek C, Vergara IA, Pires daSilva I, Allen R, et al. Intratumoral CD16+ macrophages are associated with clinical outcomes of patients with metastatic melanoma treated with combination anti-PD-1 and anti-CTLA-4 therapy. Clin Cancer Res 2023;29:2513–24.
42. Shields RL, Namenuk AK, Hong K, Meng YG, Rae J, Briggs J, et al. High resolution mapping of the binding site on human IgG1 for Fc gamma RI, Fc gamma RII, Fc gamma RIII, and FcRn and design of IgG1 variants with improved binding to the Fc gamma R. J Biol Chem;276:6591–604.
43. Sharabi A, Tsokos MG, Ding Y, Malek TR, Klatzmann D, Tsokos GC. Regulatory T cells in the treatment of disease. Nat Rev Drug Discov 2018;17:823–44.
44. Plitas G, Konopacki C, Wu K, Bos PD, Morrow M, Putintseva EV, et al. Regulatory T cells exhibit distinct features in human breast cancer. Immunity 2016;45:1122–34.
45. De Simone M, Arrigoni A, Rossetti G, Gruarin P, Ranzani V, Politano C, et al. Transcriptional landscape of human tissue lymphocytes unveils uniqueness of tumor-infiltrating T regulatory cells. Immunity 2016;45:1135–47.
46. Campbell JR, McDonald BR, Mesko PB, Siemers NO, Singh PB, Selby M, et al. Fc-optimized anti-CCR8 antibody depletes regulatory T cells in human tumor models. Cancer Res 2021;81:2983–94.
47. Van Damme H, Dombrecht B, Kiss M, Roose H, Allen E, Van Overmeire E, et al. Therapeutic depletion of CCR8 + tumor-infiltrating regulatory T cells elicits antitumor immunity and synergizes with anti-PD-1 therapy. J Immunother Cancer 2021;9:e001749.
48. Kidani Y, Nogami W, Yasumizu Y, Kawashima A, Tanaka A, Sonoda Y, et al. CCR8-targeted specific depletion of clonally expanded Treg cells in tumor tissues evokes potent tumor immunity with long-lasting memory. Proc Natl Acad Sci U S A 2022;119:e2114282119.
49. Luoma AM, Suo S, Williams HL, Sharova T, Sullivan K, Manos M, et al. Molecular pathways of colon inflammation induced by cancer immunotherapy. Cell 2020;182:655–71.